

# Polymer Chain Behavior in Polymer Nanocomposites with Attractive Interactions

Nicolas Jouault,<sup>\*,†,‡</sup> Michael K. Crawford,<sup>\*,§</sup> Changzai Chi,<sup>§</sup> Robert J. Smalley,<sup>§</sup> Barbara Wood,<sup>§</sup> Jacques Jestin,<sup>||</sup> Yuri B. Melnichenko,<sup>⊥</sup> Lilin He,<sup>⊥</sup> William E. Guise,<sup>§,#</sup> and Sanat K. Kumar<sup>\*,‡</sup>

<sup>†</sup>Sorbonne Universités, UPMC Univ Paris 06, CNRS, Laboratoire PHENIX, Case 51, 4 place Jussieu, F-75005 Paris, France

<sup>‡</sup>Department of Chemical Engineering, Columbia University, New York, New York 10027, United States

<sup>§</sup>DuPont Central Research and Development, E400/5424, Wilmington, Delaware 19803, United States

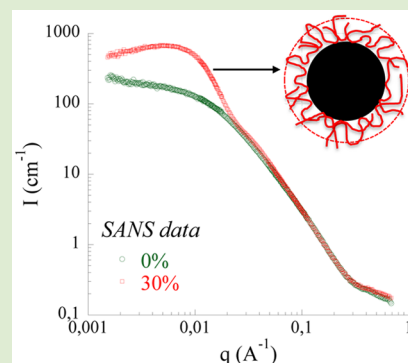
<sup>||</sup>Laboratoire Léon Brillouin (LLB), CEA Saclay, 91191 Gif-Sur-Yvette, France

<sup>⊥</sup>Biology and Soft Matter Division, Oak Ridge National Laboratory, Oak Ridge, Tennessee 37831-6393, United States

<sup>#</sup>Advanced Photon Source, Argonne National Laboratory, 9700 South Cass Avenue, Lemont, Illinois 60439, United States

## Supporting Information

**ABSTRACT:** Chain behavior has been determined in polymer nanocomposites (PNCs) comprised of well-dispersed 12 nm diameter silica nanoparticles (NPs) in poly(methyl methacrylate) (PMMA) matrices by Small-Angle Neutron Scattering (SANS) measurements under the Zero Average Contrast (ZAC) condition. In particular, we directly characterize the bound polymer layer surrounding the NPs, revealing the bound layer profile. The SANS spectra in the high- $q$  region also show no significant change in the bulk polymer radius of gyration on the addition of the NPs. We thus suggest that the bulk polymer conformation in PNCs should generally be determined using the high  $q$  region of SANS data.



Polymer nanocomposites (PNCs), that is, NP/polymer mixtures, are known to have enhanced properties relative to the neat polymer. Perhaps the most fundamental question in this area, which has the largest impact on properties, is how the polymer radius of gyration ( $R_g$ ) is affected by the NPs. The answer to this question is unclear since there have been reports of swelling,<sup>1,2</sup> contraction,<sup>3</sup> or no change<sup>4–8</sup> of polymer conformation. In particular, we ask if the precise nature of each system, specifically the sign and strength of the polymer–NP interaction, together with the NP radius ( $R_{NP}$ ) and dispersion quality, can account for these differences in behavior. To date, studies which report increases in polymer radius of gyration ( $R_g$ ) in the presence of spherical NPs, invoke the presence of attractive NP/polymer interactions, combined with  $R_{NP} < R_g$  and good NP dispersion,<sup>9</sup> to conclude that the NPs behave as good solvents for the polymer chains. All other studies on spherical NPs showed little if any changes in polymer  $R_g$ , that is, (a) where  $R_{NP} > R_g$ <sup>3</sup> or the NP–polymer interactions are believed to be athermal,<sup>7</sup> or (b) significant NP aggregation was present<sup>10</sup> due to unfavorable NP/polymer interactions. While these are physically motivated arguments, another possibility for the variability in the results comes from experimental artifacts. Chain conformations in PNCs have been primarily measured by small-angle neutron scattering (SANS). This measurement is greatly facilitated by combining deuterated and hydrogenated chains such that the average

scattering length density (SLD) of the polymer mixture closely matches the SLD of the silica. This Zero Average Contrast (ZAC) condition<sup>11</sup> minimizes the scattering due to the NPs. Under this assumption, this ZAC measurement is uniquely sensitive to the form factor of the chains without interference from polymer structure factors. However, the rigorous ZAC condition is not easily met. Many SANS studies show scattering intensity in addition to that expected from the polymer chains at low scattering vector  $q$ : this has been attributed to SLD mismatch,<sup>4</sup> H/D polymer demixing,<sup>6</sup> polymer voids,<sup>3</sup> or preferential D (or H) chain adsorption onto the NPs.<sup>8,12</sup>

This Letter focuses on analyzing the low  $q$  region in SANS data from such nominally ZAC mixtures, for a nanocomposite system (PMMA/silica) with attractive NP/polymer interactions. Our data show the clear scattering signature of the polymer bound layer, which arises due to a SLD different from the bulk polymer matrix, either due to H or D enrichment or a modification of the polymer density in the bound layer compared to the surrounding polymer matrix, as suggested by Banc and co-workers.<sup>8</sup> However, at high  $q$ , where the chain form factor scattering dominates, the conformation of polymer

Received: February 25, 2016

Accepted: April 5, 2016

Published: April 7, 2016

Table 1. Hydrogenated (H) and Deuterated (D) PMMA Used in This Study<sup>a</sup>

samples (K)	$M_w$ (kg/mol or K)		$M_w/M_n$		$R_{g,0}$ (nm)		Flory–Huggins $\chi$ parameter	$R_{NP}/R_{g,0}$ (with $R_{NP} = 6.1$ nm)	
	H PMMA	D PMMA	H PMMA	D PMMA	H PMMA	D PMMA		H PMMA	D PMMA
50	54.5	53	1.09	1.09	6.1	6.0	$8 \times 10^{-4}$	1.00	1.02
100	115	136	1.09	1.10	9.2	10.0	$3.5 \times 10^{-4}$	0.66	0.61
200	207.4	230	1.02	1.07	12.3	13.0	$2.5 \times 10^{-4}$	0.50	0.47

<sup>a</sup>All polymers were syndiotactic rich, except for the 50 and 100 K H-PMMA, which were atactic.  $R_{g,0}$  are the radii of gyration for the pure polymers that were determined by fitting the SANS data with the RPA model.

molecules in the surrounding polymer matrix is still accessible, although accurate background subtraction and data normalization is required to reliably extract it.

We focus on  $2R_{NP} = 12$  nm diameter silica NPs well dispersed in poly(methyl methacrylate) (PMMA) matrices of different molecular weights covering the range of  $R_{NP}/R_g = 0.47$ – $1.02$  (Table 1). The silica/PMMA interaction is attractive due to H-bonds between the PMMA ester group and the silanols.<sup>13,14</sup> Note that we focus on the 100 K systems in the main text and report the other  $M_w$  results in the SI. PNCs with well-dispersed NPs (Figure 1) were prepared by solvent casting

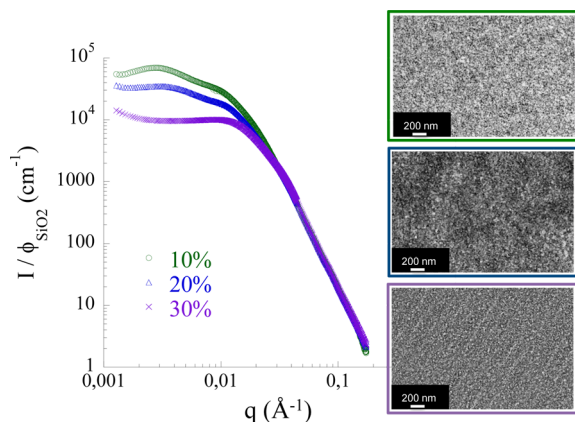


**Figure 1.** Normalized SAXS scattering intensities  $I/\phi_{\text{SiO}_2}$  (left) and TEM images (right) for 100 K PMMA/silica PNCs filled at 10% (green circles), 20% (blue triangles), and 30% v/v (purple crosses).

from dimethylacetamide (DMAc). These as-cast samples were dried under  $N_2$  at progressively higher temperatures to 155 °C for 72 h, hot pressed at 150 °C to form the SANS samples (1 mm thick  $\times$  2 cm diameter) and then additionally annealed for 64 h at 150 °C. Small-angle X-ray scattering (SAXS) and transmission electron microscopy (TEM) were used to characterize NP dispersion. SAXS data were collected over  $q = 0.002$ – $0.5 \text{ \AA}^{-1}$  on an insertion device beamline at the DND-CAT sector of the Advanced Photon Source (APS) at Argonne National Laboratory.

Figure 1 shows SAXS results normalized by silica volume fraction  $\phi_{\text{SiO}_2}$  for 100 K PMMA PNCs. The data show a  $q^{-4}$  dependence at large  $q$  characteristic of sharp NP/polymer interfaces. At low  $q$ , the 10% data can be fitted with an aggregate form factor<sup>15</sup> with an average aggregation number  $N_{\text{agg}}$  of 1.7. Thus, the NPs mostly arrange in very small aggregates. A correlation peak is also observed, arising from the repulsion between the NP aggregates. At higher NP volume fraction (20 and 30% v/v) this correlation peak's position moves to higher  $q$ .<sup>15</sup> The location of the peaks ( $q^*$ ) gives the average mesh size of the silica network  $d$ , where  $d = 2\pi/q^*$ .

However, the tendency for NP aggregation is more pronounced for lower  $M_w$  polymer (see Figure S4). As shown previously, silica NPs are charged in DMAc, and electrostatic repulsion prevents NP aggregation.<sup>16</sup> However, when the solvent evaporates, this charge stabilization is rapidly lost, and the increase of the solution viscosity kinetically prevents aggregation. High molecular weights experience more rapidly increasing viscosities during solvent evaporation, leading to more uniform dispersion.<sup>16,17</sup>

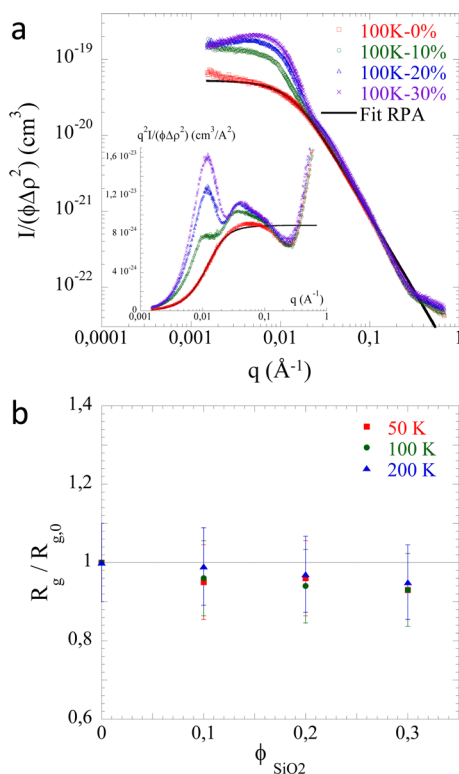
The same samples were then studied by SANS to determine polymer conformations. SANS data were collected on beamlines CG-2 and CG-3 at the High Flux Isotope Reactor at Oak Ridge National Laboratory (Oak Ridge, Tennessee, U.S.A.; see SI). By combining 59.5% v/v H-PMMA, with a scattering length density (SLD) of  $1.06 \times 10^{10} \text{ cm}^{-2}$ , and 40.5% v/v D-PMMA, with  $\text{SLD} = 6.97 \times 10^{10} \text{ cm}^{-2}$ , we create a mixture ( $\text{SLD} = 3.45 \times 10^{10} \text{ cm}^{-2}$ ) with essentially the SLD of the NPs ( $3.48 \times 10^{10} \text{ cm}^{-2}$ , see Figure S2); this should eliminate scattering from the NPs and interchain correlations. The influence of the small SLD mismatch is discussed below. The SANS background comes from the incoherent scattering: we have measured pure H-PMMA (see Figure S3) and D-PMMA values are from O'Reilly et al.;<sup>18</sup> the silica has practically no scattering. From here,  $I(q) = 0.348 \text{ cm}^{-1}$  was subtracted from the polymer contribution to the PNC scattering.

Figure 2a shows the scattering intensity of 100 K PMMA PNCs under the ZAC condition, normalized by  $\phi\Delta\rho^2$  ( $\phi = \phi_{\text{PMMA}}\phi_{\text{H}}(1 - \phi_{\text{H}})$ , with  $\phi_{\text{PMMA}}$  the total polymer volume fraction,  $\phi_{\text{H}}$  the H-PMMA volume fraction, and  $\Delta\rho^2 = (\rho_{\text{H-PMMA}} - \rho_{\text{D-PMMA}})^2$  the contrast term), as a function of  $q$  for different PNCs. The inset shows the Kratky representation,  $q^2 I/\phi\Delta\rho^2$ , as a function of  $q$ .

For pure PMMA, the intensity is well fitted by the RPA expression (see results in Table 1) up to a  $q = 0.065 \text{ \AA}^{-1}$ , where a maximum is visible. Previous works<sup>18,19</sup> clearly show that the SANS data up to the maximum are well fitted by the Gaussian chain form factor. The features at higher  $q$  values reflect the specific chain tacticity.<sup>20</sup> We shall therefore use the Kratky intensity values at the maximum ( $q = 0.065 \text{ \AA}^{-1}$ ),  $q^2 I(q)/(\phi\Delta\rho^2)$ , to determine PMMA chain dimensions. When adding silica NPs, the Kratky intensity at the peak position,  $q^2 I/\phi\Delta\rho^2$ , is slightly increased, and one can extract  $R_g/R_{g,0}$ :

$$\frac{R_g}{R_{g,0}} = \sqrt{\frac{q^2 I/(\phi\Delta\rho^2)}{q^2 I_0/(\phi\Delta\rho^2_0)}}$$

We thus obtain  $R_g/R_{g,0} = 0.96, 0.94,$  and  $0.93$  for 10, 20, and 30% v/v silica NPs, respectively (Figure 2b). Within the experimental error of 10% there is thus no significant change of  $R_g$ , in direct contrast to some earlier results.<sup>1,2</sup> Previous works suggested significant chain swelling in the presence of small NPs and attractive interactions. In our study, the presence of a



**Figure 2.** (a) Normalized SANS scattering intensities  $I/\phi\Delta\rho^2$  (with  $\phi = \phi_{\text{PMMA}}\phi_{\text{H}}(1 - \phi_{\text{H}})$ ) of 100 K PMMA PNCs filled with 0, 10, 20, and 30% v/v of silica NPs. The inset shows the Kratky representation. The continuous black line is the best fit using the RPA expression. (b)  $R_g/R_{g,0}$  as the function of silica volume fraction  $\Phi_{\text{SiO}_2}$  extracted from the SANS high  $q$  region for the different PMMA  $M_w$ s (see main text). The experimental error bars are  $\pm 10\%$  (uncertainties from the SANS instrument).

bound layer may (i) screen the bulk polymer from the NPs returning the system to the athermal limit and (ii) increase the effective size of the NPs. These combined effects may explain the measured unchanged conformation. Our results are similar to the observations of Nusser et al. on poly(ethylene-propylene)/silica PNCs with no attractive polymer/NP interaction (with  $R_{\text{NP}} \approx R_g$ ).<sup>3</sup> This is the first important message: there are no significant changes in  $R_g$  in PNCs with both  $R_{\text{NP}} < R_g$  and attractive NP/polymer interactions, independent of the polymer molecular weight (see Figure 2b).

At low  $q$ , an additional scattering intensity is clearly visible as a peak for all silica volume fractions, making  $R_g$  determination difficult using the RPA or Guinier methods. The origin of this extra scattering<sup>3,5,8</sup> is unexpected since we are working near the ZAC condition. One possibility is that the small SLD mismatch between the NP and polymer leads to scattering at low  $q$ . To evaluate this interpretation, SANS and SAXS spectra were compared in Figure 3 for PNCs composed of 100 K PMMA and 30% NPs.

Figure 3 shows that the location of the maxima in the SANS data does not agree with the SAXS maxima. To go further, we calculated the scattering  $I_{\text{calcd}}$  due to our small experimental SLD mismatch (Figure 3, here the contrast term is  $\Delta\rho_{\text{SANS-mismatch}}^2 = (3.48 - 3.45)^2 \times 10^{20} = 9 \times 10^{16} \text{ cm}^{-4}$ ); this is clearly negligible (around  $0.1 \text{ cm}^{-1}$  at low  $q$ ). We then combined the pure PMMA SANS signal,  $I_{\text{pure PMMA}}$  (i.e., the 0%

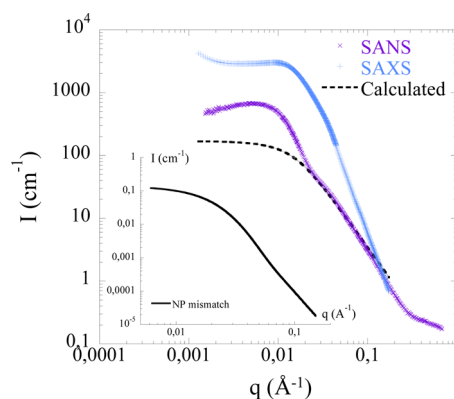


**Figure 3.** SANS and SAXS comparison of the scattering intensity for 30% v/v 100 K PMMA PNC. The dash line is a theoretical calculation of the scattering intensity due to a silica mismatch. The inset shows the NP form factor calculated using our experimental mismatch.

NP sample) with the SAXS scattering intensity,  $I_{\text{SAXS}}$ , as follows:

$$I_{\text{calcd}} = (q) \left( \frac{\Delta\rho_{\text{SANS-mismatch}}^2}{\Delta\rho_{\text{SAXS}}^2} \right) I_{\text{SAXS}} + (1 - \Phi_{\text{SiO}_2}) I_{\text{pure PMMA}}$$

where  $\Delta\rho_{\text{SAXS}}^2$  is the SAXS contrast ( $=71.4 \times 10^{20} \text{ cm}^{-4}$ ). This result (black dashed line in Figure 3) also does not reproduce our SANS data at low  $q$ . Thus, the extra scattering is clearly not due to NP/polymer scattering contrast mismatch. Since the additional SANS scattering peak is located at slightly lower  $q$  than the SAXS, we propose that it arises from the presence of a bound polymer layer at the silica surface, creating a SLD contrast despite the fact that the ZAC condition is fulfilled on average.<sup>8</sup> Such a contrast can arise from a preferential adsorption of H or D chains and a different polymer density of the bound layer compared to the PMMA matrix.<sup>21,22</sup>

To test this hypothesis, we plot  $I(q)_{\text{bound layer}} = I(q)_{\text{PNC}} - (1 - \phi_{\text{SiO}_2})I(q)_{\text{neat PMMA}}$ , the extra contribution due to the bound layer (see Figure 4a). A spherical core-shell model with an exponential diffuse SLD shell profile<sup>23</sup> is then used to fit the data using the SASfit program.<sup>24</sup> The free parameters of the fit are the core radius  $R_c$  and polydispersity  $\sigma$ , the pure bound layer SLD and the bulk SLD (see details in SI). All other parameters were fixed: volume fraction, core SLD ( $3.48 \times 10^{10} \text{ cm}^{-2}$ ), and shell thickness  $e$  equal to the  $R_g$  of the polymer, as observed recently.<sup>25</sup> One can see in Figure 4 and Table 2 that  $I_{\text{bound layer}}(q)$  is well reproduced by this model. At low  $q$ , the data show a maximum (visible for 30% v/v), whose position does not match with the SAXS correlation peak (see Figure 3). Since the bound layer center of mass is the same as the NPs, the intershell structure factor should be similar to the NP structure factor.<sup>26</sup> This discrepancy may arise from the subtraction of pure PMMA signal described above.

At 10% v/v, the  $R_c$  value extracted from the fit is in good agreement with the one derived from SAXS data. For 20% and 30% v/v, the fits give a core radius of 9.8 and 9.6 nm, respectively. Contrary to SAXS, which is not sensitive to deuteration, the SANS data reveal that polymer surrounds small NP aggregates. The bound layer SLDs are different from the ZAC SLD. Since we cannot distinguish between higher or lower bound layer SLD, we present in Table 2 the difference between the bound layer SLD and the ZAC SLD,  $|\Delta\rho_{\text{bound layer}}|$ . This difference reflects the fact that the layer SLD can be above

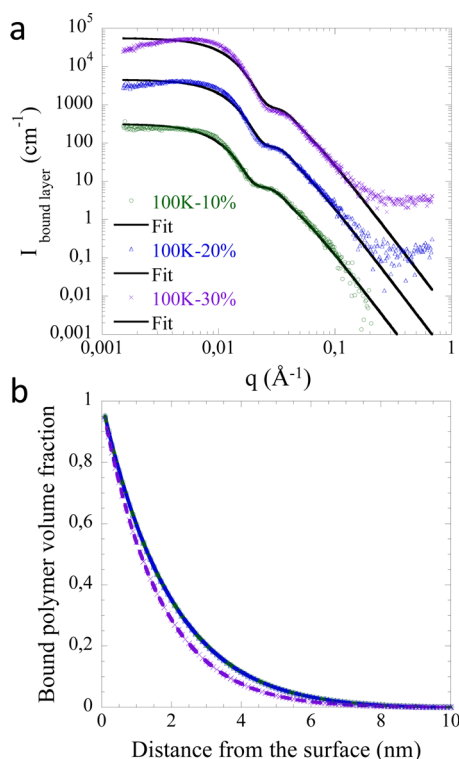


**Figure 4.** (a) Bound layer scattering intensities  $I(q)_{\text{bound layer}} = I(q) - (1 - \phi_{\text{SiO}_2}) \times I(q)_{\text{pure PMMA}}$  for 10% (green circles), 20% (blue triangles), and 30% v/v (purple crosses) 100 K PMMA PNCs. The 20% and 30% v/v curves have been shifted for clarity by factors of 10 and 100, respectively. (b) Bound polymer volume fraction profiles obtained by converting the shell SLDs.

**Table 2. Free Parameters for the Fits of the Bound Layer Scattering Intensities Shown in Figure 4a**

silica volume fraction (%)	core radius $R_c$ nm/ $\sigma$	$ \Delta\rho_{\text{bound layer}} $ ( $\times 10^{10} \text{ cm}^{-2}$ )	$ \Delta\rho_{\text{bulk}} $ ( $\times 10^{10} \text{ cm}^{-2}$ )
10	11.5/0.28	1.04	0
20	9.8/0.28	1.08	0.03
30	9.6/0.28	1.08	0.07

or below the ZAC SLD, suggesting either H or D enrichment<sup>27,28</sup> or a modification of the polymer density at the surface.<sup>22</sup> Similarly, the differences between the bulk SLD and the ZAC SLD,  $|\Delta\rho_{\text{bulk}}|$ , are presented and are low: the resulting bulk PMMA SLD is still comparable to the NP SLD, so the mismatch remains negligible. More importantly, the fits determine the exponential SLD profiles, that is, the changes of the bound layer SLDs with distance from the NP interface. These SLD profiles are then converted into the bound layer volume fraction profiles shown in Figure 4b. First, the profiles appear independent of silica volume fraction, suggesting no compression of the bound layer. Then, as observed by Koga et al.,<sup>29</sup> the bound layer volume fraction is larger at the surface (this region is mostly composed of loops) and decreases at larger distances as the bound layer becomes more diffuse due to the contribution from the tails. One can define the bound layer thickness as the distance where  $\phi_{\text{bound layer}} = 0.5$  and a value of 1.5 nm is found, in good agreement with recent results using a similar approach.<sup>8</sup> However, this thickness value is a simplification because it does not completely describe the complex chain behavior:<sup>30</sup> the profiles clearly show that the

adsorbed chains extend to larger distances, around 8 nm, which are close to the polymer  $R_g$  of 9.8 nm. This chain extension is important since it is responsible for the long-range interaction between the NPs.<sup>25</sup>

Finally, the second main message of this Letter is that the extra SANS scattering at low  $q$  can be accounted for by the existence of bound polymer layers. As a consequence of the extra low  $q$  scattering, we believe that the high  $q$  region is more appropriate to determine the bulk chain conformation. Similar analyses have been performed on 50 and 200 K PMMA, giving similar results (see Figures S4–S6). The extra scattering becomes less pronounced with increasing polymer  $M_w$ . For high  $M_w$  polymers, the chain contribution to the scattering at low  $q$  increases, overshadowing the scattering from the bound layers and making a detailed analysis more difficult (especially for the 200 K PMMA).

## ■ ASSOCIATED CONTENT

### Supporting Information

The Supporting Information is available free of charge on the ACS Publications website at DOI: 10.1021/acsmacrolett.6b00164.

Additional SANS and SAXS data, TEM images, and details on the fitting model (PDF).

## ■ AUTHOR INFORMATION

### Corresponding Authors

\*E-mail: nicolas.jouault@upmc.fr.

\*E-mail: mkcrawford987@gmail.com.

\*E-mail: sk2794@columbia.edu.

### Notes

The authors declare no competing financial interest.

## ■ ACKNOWLEDGMENTS

N.J. and S.K.K. acknowledge financial support from National Science Foundation (DMR-1408323). A portion of this research at Oak Ridge National Laboratory's High Flux Isotope Reactor was sponsored by the Scientific User Facilities Division, Office of Basic Energy Sciences, U.S. Department of Energy. Portions of this work were performed at the DuPont-Northwestern-Dow Collaborative Access Team (DND-CAT), located at Sector 5 of the Advanced Photon Source (APS). DND-CAT is supported by Northwestern University, E.I. DuPont de Nemours & Co., and The Dow Chemical Company. This research used resources of the Advanced Photon Source, a U.S. Department of Energy (DOE) Office of Science User Facility operated for the DOE Office of Science by Argonne National Laboratory under Contract No. DE-AC02-06CH11357.

## ■ REFERENCES

- (1) Nakatani, A. I.; Chen, W.; Schmidt, R. G.; Gordon, G. V.; Han, C. C. *Polymer* **2001**, *42*, 3713–3722.
- (2) Tuteja, A.; Duxbury, P. M.; Mackay, M. E. *Phys. Rev. Lett.* **2008**, *100* (7), n/a.
- (3) Nusser, K.; Neueder, S.; Schneider, G. J.; Meyer, M.; Pyckhout-Hintzen, W.; Willner, L.; Radulescu, A.; Richter, D. *Macromolecules* **2010**, *43*, 9837–9847.
- (4) Sen, S.; Xie, Y. P.; Kumar, S. K.; Yang, H. C.; Bansal, A.; Ho, D. L.; Hall, L.; Hooper, J. B.; Schweizer, K. S. *Phys. Rev. Lett.* **2007**, *98* (12), n/a.
- (5) Jouault, N.; Dalmás, F.; Said, S.; Di Cola, E.; Schweins, R.; Jestin, J.; Boue, F. *Macromolecules* **2010**, *43*, 9881–9891.

- (6) Genix, A. C.; Tatou, M.; Imaz, A.; Forcada, J.; Schweins, R.; Grillo, I.; Oberdisse, J. *Macromolecules* **2012**, *45* (3), 1663–1675.
- (7) Crawford, M. K.; Smalley, R. J.; Cohen, G.; Hogan, B.; Wood, B. A.; Kumar, S. K.; Melnichenko, Y. B.; He, L.; Guise, W.; Hammouda, B. *Phys. Rev. Lett.* **2013**, *110*, 196001.
- (8) Banc, A.; Genix, A.-C.; Dupas, C.; Sztucki, M.; Schweins, R.; Appavou, M.-S.; Oberdisse, J. *Macromolecules* **2015**, *48* (18), 6596–6605.
- (9) Karatrantos, A.; Clarke, N.; Composto, R. J.; Winey, K. I. *Soft Matter* **2015**, *11* (2), 382–388.
- (10) Bouty, A.; Petitjean, L.; Chatard, J.; Matmour, R.; Degrandcourt, C.; Schweins, R.; Meneau, F.; Kwasniewski, P.; Boue, F.; Couty, M.; Jestin, J. *Faraday Discuss.* **2016**, DOI: [10.1039/C5FD00130G](https://doi.org/10.1039/C5FD00130G).
- (11) Benmouna, M.; Hammouda, B. *Prog. Polym. Sci.* **1997**, *22* (1), 49–92.
- (12) Genix, A.-C.; Oberdisse, J. *Curr. Opin. Colloid Interface Sci.* **2015**, *20*, 293–303.
- (13) Kulkeratiyut, S.; Kulkeratiyut, S.; Blum, F. D. *J. Polym. Sci., Part B: Polym. Phys.* **2006**, *44* (15), 2071–2078.
- (14) Madathingal, R. R.; Wunder, S. L. *Langmuir* **2010**, *26* (7), 5077–5087.
- (15) Jouault, N.; Dalmas, F.; Boue, F.; Jestin, J. *Polymer* **2012**, *53* (3), 761–775.
- (16) Meth, J. S.; Zane, S. G.; Chi, C. Z.; Londono, J. D.; Wood, B. A.; Cotts, P.; Keating, M.; Guise, W.; Weigand, S. *Macromolecules* **2011**, *44* (20), 8301–8313.
- (17) Jouault, N.; Zhao, D.; Kumar, S. K. *Macromolecules* **2014**, *47* (15), 5246–5255.
- (18) O'Reilly, J. M.; Teegarden, D. M.; Wignall, G. D. *Macromolecules* **1985**, *18*, 2747–2752.
- (19) Dettenmaier, M.; Maconnachie, A.; Higgins, J. S.; Kausch, H. H.; Nguyen, T. Q. *Macromolecules* **1986**, *19*, 773–778.
- (20) Yoon, D. Y.; Flory, P. J. *Macromolecules* **1976**, *9* (2), 299–303.
- (21) Hooper, J. B.; Schweizer, K. S. *Macromolecules* **2007**, *40* (19), 6998–7008.
- (22) Cheng, S.; Holt, A. P.; Wang, H.; Fan, F.; Bocharova, V.; Martin, H.; Etampawala, T.; White, B. T.; Saito, T.; Kang, N.-G.; Dadmun, M. D.; Mays, J. W.; Sokolov, A. P. *Phys. Rev. Lett.* **2016**, *116* (3), 038302.
- (23) Berndt, I.; Pedersen, J. S.; Lindner, P.; Richtering, W. *Langmuir* **2006**, *22* (1), 459–468.
- (24) <https://kur.web.psi.ch/sans1/SANSSoft/sasfit.html>.
- (25) Jouault, N.; Moll, J. F.; Meng, D.; Windsor, K.; Ramcharan, S.; Kearney, C.; Kumar, S. K. *ACS Macro Lett.* **2013**, *2* (5), 371–374.
- (26) Kim, S. Y.; Schweizer, K. S.; Zukoski, C. F. *Phys. Rev. Lett.* **2011**, *107* (22), 225504.
- (27) Hopkinson, I.; Kiff, F. T.; Richards, R. W.; Affrossman, S.; Hartshorne, M.; Pethrick, R. A.; Munro, H.; Webster, J. R. P. *Macromolecules* **1995**, *28* (2), 627–635.
- (28) Hariharan, A.; Kumar, S. K.; Rafailovich, M. H.; Sokolov, J.; Zheng, X.; Duong, D.; Schwarz, S. A.; Russell, T. P. *J. Chem. Phys.* **1993**, *99* (1), 656–663.
- (29) Jiang, N.; Endoh, M. K.; Koga, T.; Masui, T.; Kishimoto, H.; Nagao, M.; Satija, S. K.; Taniguchi, T. *ACS Macro Lett.* **2015**, *4* (8), 838–842.
- (30) Semenov, A. N.; Joanny, J. F. *Europhys. Lett.* **1995**, *29* (4), 279.